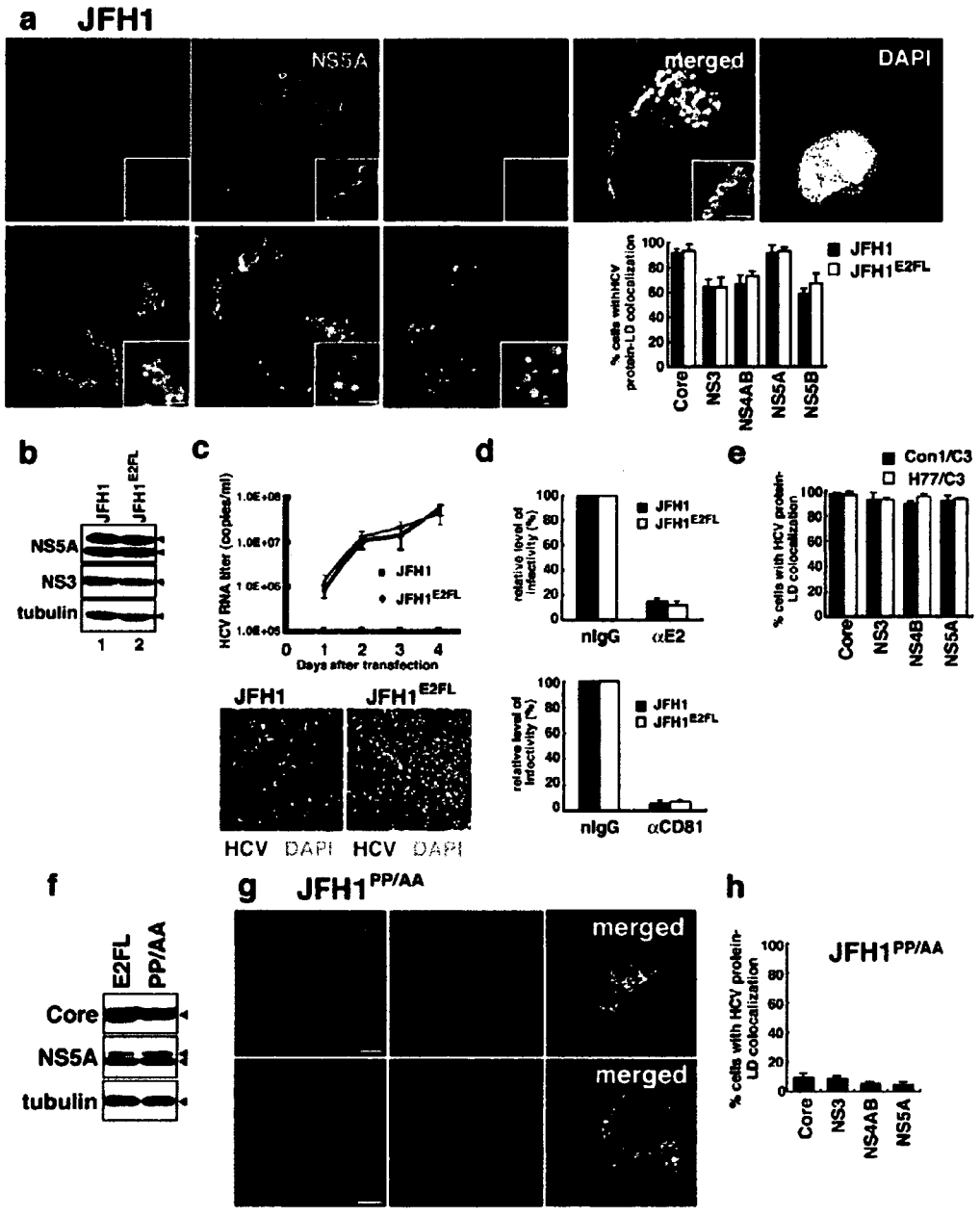


**Supplementary Fig. S2 Kunitata Shimotohno**
**NCB-S11732B**

**Supplementary Fig. 2 Characterization of mutant JFH1s**

(a) JFH1-replicating cells were stained with indicated antibodies, BODYPI 493/503 and

DAPI. Scale bars = 2 μm. Percentages of JFH1- and JFH1$^{E2FL}$-replicating cells with overlapping signals for LDs and HCV proteins (n > 200). (b) HCV proteins in JFH1 and JFH1$^{E2FL}$ replicating cells were analyzed by western blotting with indicated antibodies. (c) Efficiency of virus production and infectivity of JFH1 and JFH1$^{E2FL}$ viruses were analyzed as described in Fig. 4. (n = 3) (d) Inhibition of HCV infection by anti-E2 antibody and anti-CD81 antibody. JFH1 and JFH1$^{E2FL}$ virus were pre-incubated with normal IgG (nIgG) or anti-E2 antibody for 1 hr at 4°C and were subsequently used to inoculate Huh-7.5 cells (upper panel). Huh-7.5 cells were pre-incubated with normal IgG (nIgG) or anti-CD81 antibody for 1 hr at 37°C before inoculation with JFH1 or JFH1$^{E2FL}$ viruses (lower panel) (n = 3). No obvious difference with respect to the subcellular localization of viral proteins (a), efficiency of viral replication (b), virus production (c), and pathway of virus entry (d) were observed between JFH1$^{E2FL}$ and JFH1 (e) Con1/C3 or H77/C3 replicating cells were stained for HCV antigens (Core or NS3 or NS4B or NS5A) and LDs. The graphs show the percentage of Con1/C3 (black) or H77/C3 (white) positive cells in which HCV protein signals overlapped with LD signals. The overlapping signals were detected by using the ImageJ RG2B software package (n > 200). (f) Whole-cell extracts of JFH1$^{E2FL}$ (E2FL) and JFH1$^{PP/AA}$ (PP/AA) replicon-bearing cells were analyzed by Western blot with indicated antibodies. Both Core$^{Wt}$ and Core$^{PP/AA}$ had an apparent molecular weight of about 21 kDa, indicating that Core$^{PP/AA}$ was efficiently processed. The expression level of Core$^{PP/AA}$, however, was slightly lower than that of Core$^{Wt}$. (g) Analysis of the subcellular localization of Core and NS5A in cells bearing the JFH1$^{PP/AA}$ mutant. Cells were labeled to detect LDs (green), Core (red), NS5A (red) and nuclei DAPI (blue). Scale bars = 10μm. (h) The percentages of JFH1$^{PP/AA}$ replicon-bearing cells positive for overlapping signals of LDs and HCV proteins are indicated (n > 200).

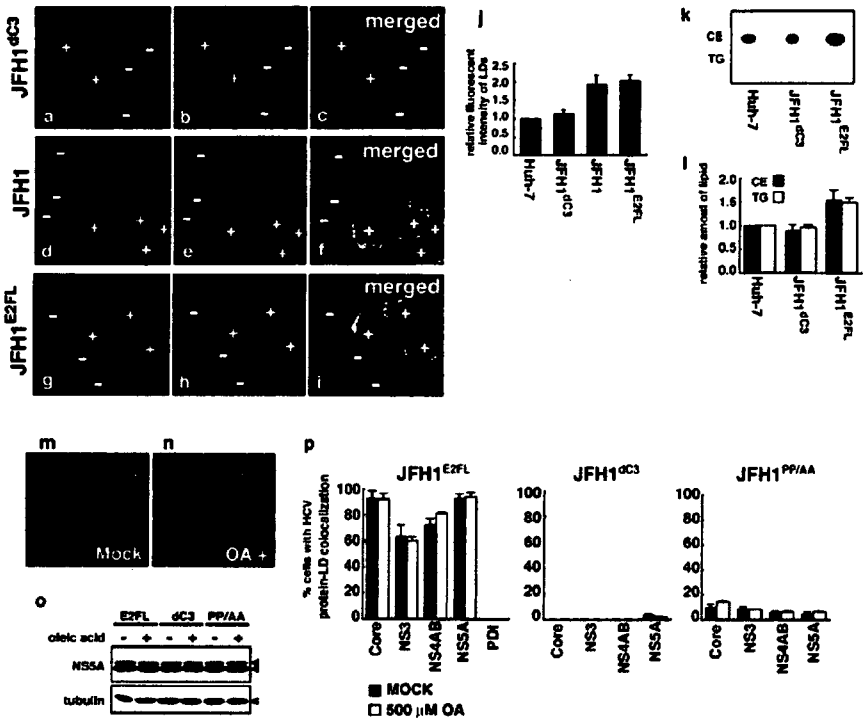


**Supplementary Fig. S3 Kunitata Shimotohno NCB-S11732B**

**Supplementary Fig. 3**

**Enhanced formation of LDs in JFH1- and JFH1$^{E2FL}$-replicating cells**

Cells transfected with JFH1$^{dC3}$ (a-c), JFH1 (d-f), and JFH1$^{E2FL}$ RNA (g-i) were stained with BODIPY493/503 (green), DAPI (blue), and anti-NS5A antibody (red). + and – indicate HCV-positive and HCV-negative cells, respectively. Fluorescence intensities of LDs in Huh-7 cells, JFH1$^{dC3}$-, JFH1-, and JFH1$^{E2FL}$-replicating cells were measured by confocal microscopy. The results are represented as relative fluorescence intensity of LDs (j). (k and l) Lipid fraction extracted from Huh-7 cells, JFH1$^{dC3}$-, and JFH1$^{E2FL}$-replicating cells was analyzed by thin-layer chromatography. Each lane was loaded with lipid corresponding to an equal amount of protein. Cholesterol ester (CE) and triglyceride (TG) are indicated (k). The relative intensity of CE and TG in panel k is shown in l (n = 3). (m-p) JFH1$^{E2FL}$ replicon-bearing cells were treated with 500 μM oleic acid for 24 hrs and were labeled with BODIPY493/503 (m and n). Cells transfected with JFH1$^{E2FL}$ (E2FL), JFH$^{dC3}$ (dC3), or JFH$^{PP/AA}$ (PP/AA) RNA were treated with or without oleic acid. (o) The HCV protein level as represented by the level of NS5A was analyzed by western blot. (p) The percentages of cells positive for overlapping signals for LDs and the HCV proteins or PDI are indicated. The data was obtained in the presence (500 μM) or absence (MOCK) of oleic acid in the culture medium (n > 200).

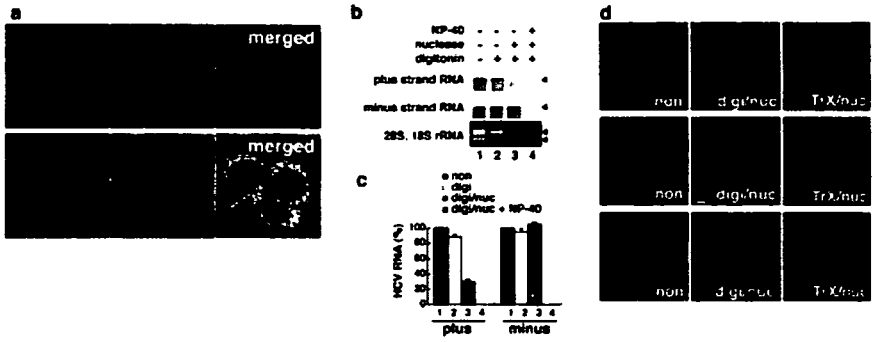


Supplementary Fig. S4 Kunitada Shimotohno
NCB-S11732B

**Supplementary Fig. 4**

**Subcellular localizations of plus- and minus-strand HCV RNA**

(a) JFH1$^{E2FL}$ replicating cells were analyzed by *in situ* hybridization to detect plus- and minus-strand HCV RNA (green). The cells were also labeled with anti-PDI antibodies (red) and DAPI (blue). Scale bars = 10 μm. (b, c) Relative amounts of plus- and minus-strand HCV RNAs. JFH1$^{E2FL}$-expressing cells were permeabilized with digitonin. The cells were treated with nuclease in the presence or absence of NP-40. Then, total RNA was analyzed by Northern blots with strand-specific HCV RNA probes. 28S and 18S ribosomal RNA was stained with ethidium bromide (b). The signals were quantified and plotted in c (n = 3). The amounts of plus- and minus-strand RNA were similar before and after digitonin treatment (lanes 1 and 2). The level of plus-strand RNA, however, was reduced by approximately 70% after nuclease treatment, whereas the level of minus-strand RNA remained constant (lanes 2 and 3). Nuclease treatment in the presence of NP-40 used to lyse the membranes caused both plus- and minus-strand HCV RNA to disappear (lane 4). This result suggests that ~30% and ~100% of plus- and minus-strand HCV RNA, respectively, are located in the replication complexes. (d) Localization of nuclease-resistant JFH1$^{E2FL}$ RNA was analyzed by *in situ* hybridization. Digitonin-permeabilized cells were treated with nuclease in the presence (TrX/nuc) or absence (digi/nuc) of Triton X-100. Total RNA was visualized with SYTO RNAselect. "non" indicates cells without digitonin and nuclease treatment. Using the nuclease-resistant HCV RNA as a marker of replication complexes, we examined the localization of the replication complexes. Both plus- and minus-strand HCV RNA were detected in the perinuclear region even after the nuclease treatment. As expected, these RNAs were no longer detectable after nuclease treatment in the presence of Triton X-100. The intensity of the plus-strand RNA signal decreased after nuclease treatment (compare upper left and middle panels). However, the intensity of the minus-strand RNA signal remained unchanged after the treatment. These results correlated with the data obtained by Northern blotting analysis. For this reason, the percentages of cells with overlapping signals for LDs and plus- or minus-strand HCV RNA (Fig. 2c) were measured after lysis of cells with digitonin and nuclease treatment. Scale bars = 10 μm.

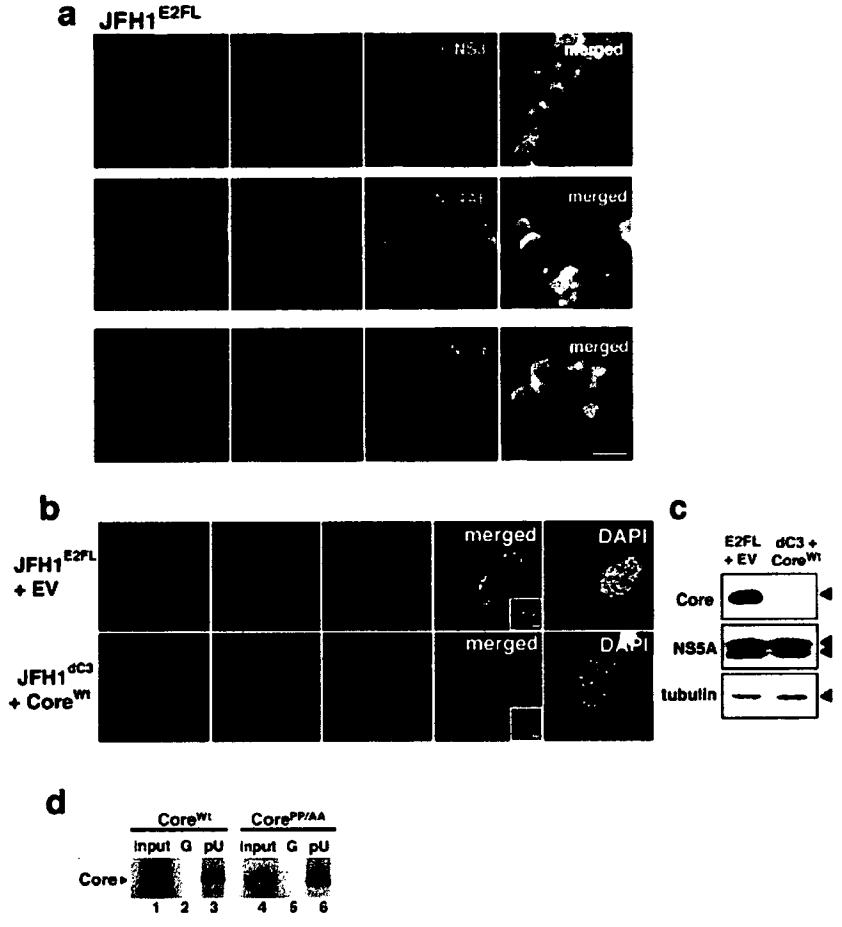


**Supplementary Fig. S5 Kunitata Shimotohno NCB-S11732B**

**Supplementary Fig. 5**

**Subcellular localization of HCV proteins in JFH1$^{E2FL}$-replicating cells and cells inoculated with rescued viruses, and RNA binding nature of Core.**

(a) JFH1$^{E2FL}$-replicating cells were labeled to detect LDs (green), Core (red), NS3 (cyan), NS4AB (cyan), and NS5B (cyan). Scale bars = 2 μm (b) The subcellular localizations of NS5A and Core in Huh-7.5 cells infected with viruses released from JFH1$^{E2FL}$ replicon-bearings cells co-transfected with pcDNA3 (upper panels) and from JFH1$^{dC3}$ replicon-bearing cells co-transfected with pcDNA3-Core$^{Wt}$ (lower panels). Cells were labeled with DAPI (white), BODIPY 493/503 (green), anti-Core (blue), and anti-NS5A (red) antibodies. The insets are high magnifications of the corresponding panel. (c) HCV proteins from these infected cells were analyzed by western blotting. (d) An RNA-protein binding precipitation assay was performed with *in vitro*-translated and $^{35}$S-radiolabeled Core$^{Wt}$ (lane 1-3) and Core$^{PP/AA}$ (lane 4-6). The resulting precipitates were analyzed by SDS-PAGE and detected by autoradiography. "G" and "pU" mark samples obtained using protein G Sepharose and poly-U Sepharose as the resin, respectively. "input" indicates 1/20 of the amount of translated product used in this assay.

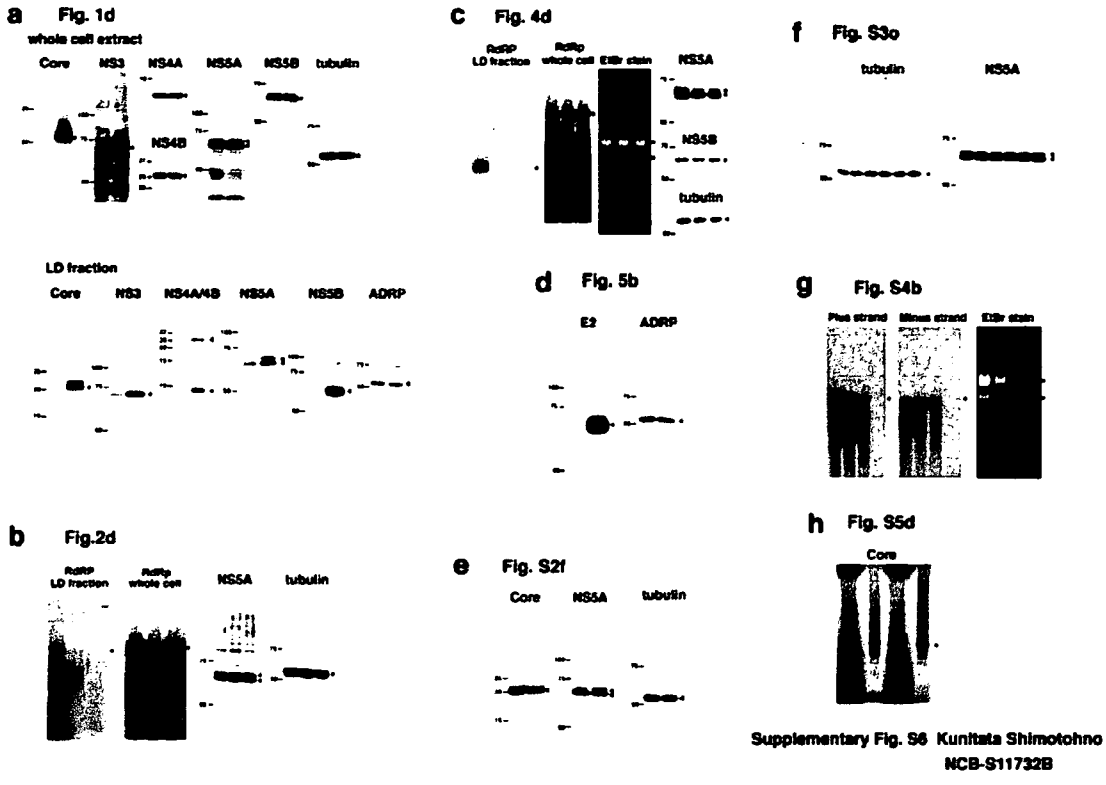


**Supplementary Fig. 6**

**Full scan of key gel images depicted in the individual figures.**

Full scans of (a) immunoblot detection of whole cell extract and LD fraction from JFH1$^{E2FL}$- and JFH1$^{dC3}$-replicating cells shown in Fig. 1d, (b) RNA synthesis assay and immunoblot detection of JFH1$^{E2FL}$-, JFH1$^{dC3}$-, and JFH1$^{PP/AA}$-replicating cells shown in Fig. 2d, (c) RNA synthesis assay and immunoblot detection of JFH1$^{E2FL}$-, JFH1$^{AAA99}$-, and JFH1$^{AAA102}$-replicating cells shown in Fig. 4d, (d) immunoblot detection of LD fraction from JFH1$^{E2FL}$- and JFH1$^{dC3}$-replicating cells shown in Fig. 5b, (e) immunoblot detection of JFH1$^{E2FL}$- and JFH1$^{PP/AA}$-replicating cells shown in Fig. S2f, (f) immunoblot detection of JFH1$^{E2FL}$-replicating cells shown in Fig. S3o, (g) Northern Blotting analysis of JFH1$^{E2FL}$-replicating cells shown in Fig. S4b, and (h) RNA-protein binding precipitation assay shown in Fig. S5d. Size of molecular weight markers (kDa) is indicated at the left side of western blot gel images. *In vitro* transcribed HCV RNA was used as a size marker for RNA gel electrophoresis (b, c, and g).

| plasmid name | primer sequences (5' to 3') | template for PCR | restriction enzyme | original plasmid |
|---|---|---|---|---|
| pcDNA3 Core $^{(1)}$ | AGACCCAAGCTTCACCATGAGCACAAATCCTAAACC | pJFH1 | HindIII | pcDNA3 |
| | AATGGAATTCTCAAGCAGAGACCGGAACGGTGATGC | | EcoRI | |
| pcDNA3-TME2 | AGACCCAAGCTTCACCATGGCTCACTGGGGCGTCATGTTC | pJFH1 | HindIII | pcDNA3 |
| | AATGGAATTCTCATCCTTCCGCCCTCGCCCAACAAC | | EcoRI | |
| pcDNA3-NS3 | AGACCCAAGCTTCACCATGGCTCCCATCACTGCTTATGCC | pJFH1 | HindIII | pcDNA3 |
| | AATGGAATTCTCAGGTCATGACCTCAAGGTCAGC | | EcoRI | |
| pcDNA3-NS4B | AGACCCAAGCTTCACCATGGCCTCTAGGGCGGCTCTCATCG | pJFH1 | HindIII | pcDNA3 |
| | AATGGAATTCTCAGCATGGGATGGGGCAGTCCTC | | EcoRI | |
| pcDNA3-NS5B | CTCGGATCCACCATGTCCATGTCATACTCCTGGACC | pJFH1 | BamHI | pcDNA3 |
| | AATGGAATTCCTACCGAGCGCGGAGTAGGAAGAGG | | EcoRI | |
| pcDNA3-Core $^{PP\ AA}$ | CATGGGGTACATCGCCGTCGTAGGCGCCGCGCTTAGTGGCG | pJFH1 $^{PP\ AA}$ | HindIII | pcDNA3 |
| | CGCCACTAAGCGCGGCGACGTACGACGGCGATGTACCCCATG | | EcoRI | |
| pJFH1 $^{E2FL}$ | GATTACAAGGATGACGACGATAAGGGCGTGTTCAGCCATGGCCC | pJFH1 | BsWI | pJFH1 |
| | CTTATCGTCGTCATCCTTGTAATCAACAGCGCCTCCAACGGTGG | | NotI | |
| | GGGACATGATGATGAACTGG | | | |
| | GTAATGTCAAACACCACACC | | | |
| pJFH1 $^{E2FL}$ | GAAAAACCAAAAGAAACACCAACTATGCAACAGGGAACCTACC | pJFH1 $^{E2FL}$ | EcoRI | pJFH1 $^{E2FL}$ |
| | GTTGGTGTTTCTTTTGGTTTTTC | | BsWI | |
| | GGGACATGATGATGAACTGG | | | |
| | GTAATGTCAAACACCACACC | | | |
| pJFH1 $^{PP\ AA}$ | CATGGGGTACATCGCCGTCGTAGGCGCCGCGCTTAGTGGCG | pJFH1 $^{E2FL}$ | EcoRI | pJFH1 $^{E2FL}$ |
| | CGCCACTAAGCGCGGCGACGTACGACGGCGATGTACCCCATG | | BsWI | |
| | GGGACATGATGATGAACTGG | | | |
| | GTAATGTCAAACACCACACC | | | |
| pJFH1 $^{E2FL}$ dBamHI | TACTGCCTGGCATCCTGTCTCC | pJFH1 $^{E2FL}$ | NsiI | pJFH1 $^{E2FL}$ |
| | CGACACAGGATGCCAGGCAGTA | | RsrII | |
| | CTATTACCAATGAGGTCACC | | | |
| | GAACAATTTAGAGGTCAGCC | | | |
| pJFH1 $^{AAA(8)}$ | GGCCAGTGCGCGGCGGCACCCCCCACG | pJFH1 $^{E2FL}$ | BamHI | pJFH1 $^{E2FL}$ dBamHI |
| | CGTGGGGGGTGCCGCCGCGCACTGGCC | | RsrII | |
| | TGGATGAACAGGCTTATTGC | | | |
| | GGTTGAAGCTCTACCTGATC | | | |
| pJFH1 $^{AAA(12)}$ | GCGCGGAAAGCCGCCGCGAACTACAAG | pJFH1 $^{E2FL}$ | BamHI | pJFH1 $^{E2FL}$ dBamHI |
| | CTTGTAGTTCGCGCCGCGCTTTCCGCGC | | RsrII | |
| | TGGATGAACAGGCTTATTGC | | | |
| | GGTTGAAGCTCTACCTGATC | | | |

## Supplementary Table

A list of the plasmids used in this work. The sets of primers used to amplify the target genes, the template plasmids used in the PCRs, the restriction sites, and plasmids into which the amplified DNA fragments were inserted are shown.

## *Supplementary Materials and Methods*

### Cell culture

The human hepatoma cell lines Huh-7 and Huh-7.5[1] were grown in Dulbecco's modified Eagle's medium (DMEM; Invitrogen, CA, USA) supplemented with 10% fetal bovine serum (FBS), 100 U/ml nonessential amino acids (Invitrogen), and 100 μg/ml penicillin and streptomycin sulfate (Invitrogen). Huh-7.5 cells were obtained from Dr. C. Rice. (Rockefeller University, USA)

### Plasmid construction

All plasmids were generated by insertion of PCR-amplified fragments into expression plasmids. The plasmids, the primer sequences, templates for the PCRs, and the restriction enzyme sites used to construct the plasmids are listed in Supplementary Table 1.

### DNA and RNA transfection

Transfection of HCV RNA was performed as previously described[2]. DNA transfection was performed using Lipofectamine 2000 (Invitrogen) according to the manufacturer's instructions.

### Northern blotting

Northern blot analysis was performed as described previously[3] with strand specific RNA probes.

### RT-PCR analysis

Quantitative real-time RT-PCR analysis of the HCV RNA titer was performed as described previously[4].

### ELISA for the detection of Core

Core in the culture medium was quantified with an ELISA according to the manufacturer's protocol (HCV antigen ELISA test, Ortho-Clinical Diagnostics).

### Thin-layer chromatography

Lipid samples extracted from cells were dissolved in chloroform methanol and were

subjected to thin-layer chromatography with a high-performance TLC plate (Merck) by the two-step method[5]. The plate was charred by a copper acetate phosphoric acid solution at 180°C.

***In vitro* transcription**

RNA for transfection was synthesized using MEGAscript T7 (Ambion, TX, USA). Plasmids carrying the JFH1 RNA sequence were linearized with *Xba*I and used as templates for transcription. Probes for *in situ* hybridization were synthesized using MAXIscript Sp6 or T7 (Ambion) in the presence of the DIG RNA labeling mix (Roche). Probes for Northern blots were synthesized with MAXIscript Sp6 or T7 in the presence of 1.85 MBq of [$\alpha$-$^{32}$P] UTP (Amersham Biosciences). For detection of plus-strand HCV RNA, minus-strand RNA probes were generated using pcDNA3-TME2 (*Hin*dIII for linearization), pcDNA3-NS3 (*Hin*dIII), and pcDNA3-NS5B (*Bam*HI) as templates for *in vitro* transcription. For detection of minus-strand HCV RNA, plus-strand RNA probes were generated using pcDNA3-TME2 (*Eco*RI), pcDNA3-NS3 (*Xba*I), and pcDNA3-NS5B (*Bam*HI) as templates. The RNA probes used for *in situ* hybridization were subjected to alkaline hydrolysis to generate fragments of ~170 nucleotides in length. Synthesized RNA probes were treated with DNase I (Ambion) and size fractionated using MicroSpin G-50 columns (Amersham Biosciences).

**Sucrose density gradient centrifugation of culture medium**

The 100-time concentrated medium from JFH1-bearing cells was loaded onto 20-50% [w/v] sucrose gradient containing 50 mM Hepes-KOH (pH 7.4), 100 mM NaCl and 1mM EDTA followed by centrifugation at 100,000 x g for 16 hrs using RPS40T rotor of HITACHI ultracentrifuge. The gradient was fractionated into 31 fractions. Buoyant density of each fraction was analyzed by Abe refractometer (ATAGO Inc., Japan). Each fraction was dialyzed against serum free DMEM and was used for the infection experiment as well as quantification of Core and HCV RNA titer as described above.

**Infection experiments**

Cells were cultured in DMEM containing 5% FBS. The medium was collected and mixed with a 0.01 volume of 1 M HEPES (pH 7.4). After filtering the sample through a 0.22-μm filter (Millipore), the filtrate was concentrated by reducing the volume to

between 1/50 and 1/100 of the original volume with an Amicon Ultra-15 centrifugal filter with Ultracel-100 membrane (Millipore). Huh-7.5 cells seeded on a collagen-coated Labtech II 8-well chamber were incubated with 100 μl of the concentrated medium for 120 min. Then, the cells were washed three times with DMEM. Twenty-four hours after the inoculation, the cells were labeled with serum from HCV-infected patients to determine the infectivity level.

***In situ* hybridization analysis**

Huh-7 cells transfected with JFH1 RNA were seeded on a collagen-coated Labtech II 8-well chamber (Nunc). Three days after seeding, the cells were washed twice with PBS and fixed with fixation solution for 15 min at room temperature. Then, the cells were permeabilized with 0.05% Triton X-100 in fixation solution for 15 min at room temperature. After washing the cells twice with cold DEPC-treated PBS, the cells were incubated in 95% formamide and 0.1x SSC (1x SSC: 150 mM NaCl and 15 mM sodium citrate) for 15 min at 65°C. After chilling the chamber on ice, the cells were incubated in 100 μl of pre-hybridization solution for 60 min at room temperature. Pre-hybridization solution was composed of 50% formamide, 2x SSC, 1 μg/ml of salmon sperm DNA (sonicated to 1-2 kb pieces, Roche), 1 μg/ml of yeast tRNA (Roche), and 2 mM vanadyl ribonucleoside complex (NEB). Then, the cells were incubated in 100 μl of hybridization solution (pre-hybridization solution containing 10% dextran sulfate and 100 to 500 ng/ml of the RNA probes) for 40 hrs at 42°C. After the hybridization, the slide glass in the chamber was transferred to a bucket filled with wash solution 1 (50% formamide and 2x SSC at pH 7.4) and washed three times for 20 min at 50°C with gentle agitation. Then, the slide was washed three more times in wash solution 2 (0.1x SSC at pH 7.4) for 20 min at 50°C with gentle agitation. The slide was incubated in blocking solution for 30 min at room temperature. To detect DIG-labeled probes, sheep anti-DIG antibodies (Roche) and Alexa 488 or Alexa 568 anti-sheep IgG antibodies (Invitrogen) were used as primary and secondary antibodies, respectively. When HCV RNA, Core, and NS5A were simultaneously labeled in the same sample, anti-DIG antibodies and the Alexa-conjugated antibodies were incubated with the samples separately to avoid cross-reaction of the Alexa 488 or Alexa 568 anti-sheep IgG antibodies with mouse and rabbit IgG. Briefly, the incubation with the anti-DIG antibodies and the Alexa 488 anti-sheep IgG antibodies was performed first. After

washing with PBS followed by a second fixation procedure, the cells were incubated with anti-Core and anti-NS5A antibodies followed by Alexa 568 anti-rabbit IgG and Alexa 647 anti-mouse IgG antibodies. For treatment with nuclease, digitonin-permeabilized cells were treated with 1 μg/ml of RNase A in the presence or absence of 0.05% Triton X-100 for 15 min at 37°C. After the treatment, RNase A was inactivated by incubation with 4% formaldehyde. Then, the cells were completely permeabilized with 0.05% Triton X-100 for 5 min at room temperature.

**Statistical analysis of the recruitment of viral components to the LD**

Only the cells that have any LDs surrounded by HCV proteins, PDI, or HCV RNA were counted as positive under immunofluorescence microscopy, and those adjacent to HCV signal were not included. The obtained cell number was divided by the total number of HCV replicating cells and is shown as "% cells with HCV protein-LD colocalization". In case of the chimeras Con1/C3 and H77/C3 LD colocalization with HCV proteins was additionally analyzed by using the ImageJ RG2B software package (Rasband, W.S., ImageJ, U. S. National Institutes of Health, Bethesda, Maryland, USA, http://rsb.info.nih.gov/ij/, 1997-2006.). Approximately 200 cells were examined for each antigen.

**RNA-protein binding precipitation assay**

*In vitro* translated [$^{35}$S]-labeled products (Core$^{Wt}$ and Core$^{PP/AA}$) were incubated with poly-U or protein G Sepharose resin in 50 mM HEPES (pH7.4), 100 mM NaCl, 0.1 % NP-40, and RNase inhibitor at 4°C for 2 hrs. After five washes, resin-bound radiolabeled proteins were analyzed by gel electrophoresis followed by autoradiography.

## *Supplementary References*


1. Blight, K. J., McKeating, J. A. & Rice, C. M. Highly permissive cell lines for subgenomic and genomic hepatitis C virus RNA replication. *J Virol* **76**, 13001-14 (2002).
2. Lohmann, V. et al. Replication of subgenomic hepatitis C virus RNAs in a hepatoma cell line. *Science* **285**, 110-3 (1999).
3. Miyanari, Y. et al. Hepatitis C virus non-structural proteins in the probable membranous compartment function in viral genome replication. *J Biol Chem* **278**, 50301-8 (2003).
4. Takeuchi, T. et al. Real-time detection system for quantification of hepatitis C virus genome. *Gastroenterology* **116**, 636-42 (1999).
5. Tauchi-Sato, K., Ozeki, S., Houjou, T., Taguchi, R. & Fujimoto, T. The surface of lipid droplets is a phospholipid monolayer with a unique Fatty Acid composition. *J Biol Chem* **277**, 44507-12 (2002).
6. Pietschmann, T. et al. Construction and characterization of infectious intragenotypic and intergenotypic hepatitis C virus chimeras. *Proc Natl Acad Sci U S A* **103**, 7408-13 (2006).

# ERRATUM

In the letter by Miyanari *et al.* (*Nature Cell Biol.* **9**, 1089–1097), Kunitada Shimotohno's affiliations were incorrectly listed. His affiliations should have been listed as 1, 2 and 6.

[1]Department of Viral Oncology, Institute for Virus Research, Kyoto University, Kyoto 606-8507, Japan.
[2]Graduate School of Biostudies, Kyoto University, Kyoto 606-8507, Japan.
[6]Correspondence should be addressed to K.S. (e-mail:shimkuni@z8.keio.jp).

*Journal of General Virology* (2007), 88, 2495–2503 DOI 10.1099/vir.0.82872-0

# Robust production of infectious viral particles in Huh-7 cells by introducing mutations in hepatitis C virus structural proteins

David Delgrange,[1] André Pillez,[1] Sandrine Castelain,[1,2] Laurence Cocquerel,[1] Yves Rouillé,[1] Jean Dubuisson,[1] Takaji Wakita,[3] Gilles Duverlie[1,2] and Czeslaw Wychowski[1]

Correspondence
Czeslaw Wychowski
czeslaw.wychowski@ibl.fr

[1]CNRS-UMR 8161, IBL, Université de Lille I et Lille II, Institut Pasteur de Lille, 59021 Lille cedex, France

[2]Laboratoire de Virologie, Centre Hospitalier Universitaire-Hôpital Sud, 80054 Amiens cedex, France

[3]Department of Virology II, National Institute of Infectious Diseases, 1-23-1 Toyama, Shinjuku, Tokyo 162-8640, Japan

Recently, the characterization of a cell culture system allowing the amplification of an authentic virus, named hepatitis C virus cell culture (HCVcc), has been reported by several groups. To obtain higher HCV particle productions, we investigated the potential effect of some amino acid changes on the infectivity of the JFH-1 isolate. As a first approach, successive infections of naïve Huh-7 cells were performed until high viral titres were obtained, and mutations that appeared during this selection were identified by sequencing. Only one major modification, N534K, located in the E2 glycoprotein sequence was found. Interestingly, this mutation prevented core glycosylation of E2 site 6. In addition, JFH-1 generated with this modification facilitated the infection of Huh-7 cells. In a second approach to identify mutations favouring HCVcc infectivity, we exploited the observation that a chimeric virus containing the genotype 1a core protein in the context of JFH-1 background was more infectious than wild-type JFH-1 isolate. Sequence alignment between JFH-1 and our chimera, led us to identify two major positions, 172 and 173, which were not occupied by similar amino acids in these two viruses. Importantly, higher viral titres were obtained by introducing these residues in the context of wild-type JFH-1. Altogether, our data indicate that a more robust production of HCVcc particles can be obtained by introducing a few specific mutations in JFH-1 structural proteins.

Received 23 January 2007
Accepted 1 May 2007

## INTRODUCTION

The *Hepatitis C virus* (HCV) is the only member of the genus *Hepacivirus* of the family *Flaviviridae*. HCV is a major cause of chronic hepatitis, liver cirrhosis, hepatocellular carcinoma (Major *et al.*, 2001) as well as several extrahepatic diseases (Houghton, 1996). An estimation of about 170 million people infected with HCV worldwide has been reported (Poynard *et al.*, 2003; Thomas, 2000).

HCV is an enveloped single-strand, positive-sense RNA virus and its genome encodes a unique open reading frame that is flanked by two structured non-translated regions in 5′ and 3′ ends of HCV genome (5′NTR and 3′NTR). Mediated by an internal ribosome entry site (Tsukiyama-Kohara *et al.*, 1992), the translation of HCV RNA genome results in polyprotein synthesis that is processed by cellular and viral proteases into at least 10 structural and non-structural (NS) proteins (Grakoui *et al.*, 1993; Hijikata *et al.*, 1991). In the viral particle, HCV genomic RNA is complexed with the highly basic capsid protein. On its surface, the viral particle bears two envelope glycoproteins E1 and E2 that are anchored in the lipid bilayer. Both these proteins have been shown to accumulate in the endoplasmic reticulum (ER), where the particles are probably assembled (Op De Beeck *et al.*, 2001). A small integral membrane protein, p7, has been reported to function as an ion channel (Griffin *et al.*, 2003; Pavlovic *et al.*, 2003). Among the NS proteins NS2, NS3, NS4A, NS4B, NS5A and NS5B, which coordinate the intracellular processes of the virus life cycle, only proteins NS3 through to 5B are sufficient to support the HCV RNA replication (Lohmann *et al.*, 1999). In addition to the polyprotein, a new HCV protein with an unknown function has also been reported. The so-called F-protein (frameshift) or ARFP (alternative reading frame protein) is generated by ribosomal frameshifting into an alternative reading frame within the

capsid-coding sequence (Roussel *et al.*, 2003; Varaklioti *et al.*, 2002; Walewski *et al.*, 2001; Xu *et al.*, 2001).

Despite intensive research efforts, the HCV life cycle and host–virus interactions have been difficult to investigate due to the lack of efficient cell culture and small animal models. Nevertheless, significant progress has been made by using heterologous expression systems. Infectivity of some cDNA-derived HCV RNAs has been demonstrated in chimpanzees upon intrahepatic inoculation (Kolykhalov *et al.*, 1997; Yanagi *et al.*, 1997, 1999). Also, the development of a functional cell-based replication system allowing efficient replication of HCV subgenomic RNAs (replicons) has provided an important tool for studying the HCV RNA replication or for evaluating potential antiviral compounds (Blight *et al.*, 2000; Lohmann *et al.*, 1999). Several surrogate systems have also been developed to palliate the difficulties in studying interactions between several candidate HCV receptors and the HCV glycoproteins. Thus, retrovirus-based pseudoparticles (pp) or HCVpp has provided the first insight into HCV entry (Bartosch *et al.*, 2003; Hsu *et al.*, 2003). But the major breakthrough arose recently with the propagation of virus in a human liver hepatoma cell line, Huh-7 (Wakita *et al.*, 2005), by transfecting these cells with an RNA transcribed from a full-length cDNA cloned initially from a patient with a fulminant hepatitis and infected with a genotype 2a isolate (Kato *et al.*, 2001). Unfortunately, it was reported by this group that the efficacy of the infection was low. Subsequently, different papers reported a robust production of infectious virus obtained with a homologous chimeric FL-J6/JFH-1 (Lindenbach *et al.*, 2005) or obtained into Huh-7.5.1 cells (Zhong *et al.*, 2005), derived from a cell line (Huh-7.5) having a defect in the RIG-I pathway (Sumpter *et al.*, 2005).

In this study, a highly efficient *in vitro* infection system based on Huh-7 cell line was obtained. The transcribed genomic JFH-1 RNA was used to produce infectious virus. The viral titre was initially low; however, successive infections of naïve Huh-7 cells led to a robust production of virus. The sequencing of the viral genome revealed only a few mutations located in the E2 glycoprotein. Furthermore and based on the characterization of a 1a–2a chimeric virus, we showed by site-directed mutagenesis that 2 aa present in the C-terminal part of the capsid-coding sequence were important for the production of high titres. Consequently, a robust HCV particle production was obtained independently of the Huh-7.5.1 cells or JFH-1 recombinant viral genome.

## METHODS

**Cell culture.** Cell monolayers of human hepatoma cell line Huh-7 (Nakabayashi *et al.*, 1982) were grown in Dulbecco's modified essential medium (DMEM; Invitrogen) supplemented with 100 nmol non-essential amino acids $l^{-1}$ and 10 % fetal bovine serum (FBS).

**Antibodies.** Rat monoclonal antibody (mAb) 3/11 (Flint *et al.*, 1999), kindly provided by J. McKeating (Institute of Biomedical Research, Birmingham University, UK) was produced *in vitro* by using a MiniPerm apparatus (Heraeus) as recommended by the manufacturer. Anti-C (ACAP27) mouse mAb was kindly provided by J. F. Delagneau (Bio-Rad, Marne-La-Coquette 92430, France). Anti-E2 mouse mAb AP33 was kindly provided by A. Patel (MRC Virology Unit, Institute of Virology, Glasgow, UK). Goat anti-$\beta$-actin polyclonal antibodies were from Santa Cruz. Alexa 488-conjugated and Alexa 555-conjugated goat anti-mouse secondary antibodies were from Molecular Probes.

**Plasmid construction.** The plasmids pJFH-1 containing the full-length cDNA of JFH-1 isolate, belonging to subtype 2a (GenBank accession no. AB047639), pJFH-1/GND and pJFH-1/ΔE1-E2 were described previously (Wakita *et al.*, 2005). Individual or combined viral mutations N534K (N6), F172C and P173S (FP→CS) were introduced into the pJFH-1 plasmid by sequential PCR steps as described using the high fidelity deep vent DNA polymerase (New England Biolabs), then assembled by a second PCR amplification (Goffard *et al.*, 2005), followed by restriction digestions and ligation. The resulting plasmids were named pJFH-1/N6 (N534K) and pJFH-1/CS. The plasmid pJFH-1/CS-N6 was obtained by inserting the fragment *Bsi*W1–*Not*I obtained from pJFH-1/N6 into the plasmid pJFH-1/CS. All constructs were verified by DNA sequencing.

***In vitro* transcription.** To generate genomic HCV RNA, the plasmid pJFH-1 and derivatives were linearized at the 3′ end of the HCV cDNA with the restriction enzyme *Xba*I (New England Biolabs). Following treatment with Mung Bean Nuclease, the linearized DNAs were then precipitated overnight and resuspended in RNase-free water to a concentration of 1 μg $\mu l^{-1}$. *In vitro* transcripts were generated using Megascript (Ambion) according to the manufacturer's protocol. The *in vitro* reaction was set up and incubated at 37 °C for 4 h. To degrade the DNA template, DNase I was added and incubated for another 20 min at 37 °C. The *in vitro* transcripts were then precipitated by the addition of LiCl and the precipitates were recovered by centrifugation. The concentration of each transcript was determined by measurement of the absorbance at 260 nm. *In vitro* transcribed RNA was delivered to cells by electroporation as described previously (Kato *et al.*, 2003a). Viral stocks were obtained by harvesting cell culture supernatants at 1 week post-transfection. Secondary viral stocks were obtained by additional infections of naïve Huh-7 cells.

**Successive infections and titration of HCV RNA by RT-PCR.** Huh-7 cells were seeded at $7 \times 10^5$ cells in T25 flask and inoculated with 2 ml supernatant medium from cells transfected with the infectious JFH-1 RNA. At 24 h, the cells were supplemented with 4 ml complete DMEM. At day 3 post-infection, infected cells were trypsinized and then replated at $2 \times 10^6$ cells in a T75 flask. Indirect immunofluorescence was used to estimate the levels of infectivity of the amplified virus. In addition, for quantification of HCV RNA, the RNA was extracted from the supernatant of infected cells and titrated by quantitative real-time RT-PCR assay (RT-qPCR) (Castelain *et al.*, 2004).

**HCV RNA genome sequencing.** Five microlitre aliquots of the RNA solutions were subjected to reverse transcription with random hexamer and moloney murine leukemia virus reverse transcriptase (Superscript II; Invitrogen) at 42 °C for 1 h. PCR primers of 20-mer designated on the sequence of JFH-1 were used to amplify five fragments of HCV cDNA (nt 129–626, 467–2367, 2285–4665, 4594–7003 and 6950–9634) to cover most of the HCV genome. One microlitre of the cDNA was subjected to PCR with TaKaRa LA *Taq* polymerase (Takara Biochemicals), and PCR conditions consisted of 30 cycles each with a denaturing cycle at 95 °C for 30 s, an annealing cycle at 60 °C for 30 s and an extension cycle at 72 °C for 2 min. The sequence of each amplified DNA was determined.

**Titration of HCV cell culture (cc).** Huh-7 cells were seeded at $8 \times 10^4$ cells per well in a 24-well plate. The next day, cell supernatants of transfected or infected Huh-7 cells were serially diluted in DMEM and used to infect naïve Huh-7 cells. The inoculum was incubated for 2 h at 37 °C, washed with DMEM and then overlaid with complete DMEM. The viral titre was then determined at 3 days post-infection by indirect immunofluorescence staining of the capsid protein and expressed as focus-forming unit per millilitre (f.f.u. $ml^{-1}$) as described previously (Zhong *et al.*, 2005).

**Western blot analysis.** Cells were lysed in a buffer containing 50 mM Tris/HCl (pH 7.5), 150 mM NaCl, 5 mM EDTA, 0.5 % (v/v) Igepal and a mixture of protease inhibitors (Complete; Roche). Protein content of pre-cleared cell lysates was determined by the BCA method as recommended by the manufacturer (Sigma), using BSA as a standard. Total proteins were separated by SDS-PAGE, transferred to nitrocellulose membranes (Hybond-ECL; Amersham) by using a Trans-Blot apparatus (Bio-rad) and revealed with a specific mAb followed by goat anti-mouse or anti-rat IgG conjugated to peroxidase (Jackson Immunoresearch) and donkey anti-goat conjugated to peroxidase. The immune complexes were visualized by enhanced chemiluminescence detection (ECL; Amersham) as recommended by the manufacturer.

**Indirect immunofluorescence microscopy.** Infected Huh-7 cells grown on coverslips were fixed in 4% paraformaldehyde. Immunostaining was performed as described previously (Rouille *et al.*, 2006) using anti-C ACAP27 mouse mAbs and anti-E2 3/11 rat mAb, followed by species-specific-conjugated secondary antibodies. Image acquisition was carried out using an Axiophot 2 microscope (Zeiss) equipped with a camera. For confocal microscopy, double-label staining was performed with anti-E2 mouse mAb AP33 (IgG1) and anti-C mouse mAb ACAP27 (IgG2a) followed by Alexa 488-conjugated goat anti-mouse IgG2a and Alexa 555-conjugated goat anti-mouse IgG1. Fluorescent signals were collected with a Leica SP2 confocal microscope equipped with a PL APO ×100/1.4 immersion objective.

## RESULTS

### Production of infectious virus in Huh-7 cell line by a transcribed genomic JFH-1 RNA

In an attempt to generate higher infection titres for HCV, Huh-7 cells were electroporated with an *in vitro* transcribed genomic JFH-1 RNA (Wakita *et al.*, 2005). Transfected cells were then passaged every 5–7 days in order to maintain subconfluent cultures during the experiment. Immunofluorescence staining for capsid and E2 proteins revealed that the percentage of positive cells increased from 30 % at day 2 to 80 % at day 12, after two passages (Fig. 1a). These results suggest that the virus spread within the cell culture allowing the untransfected cells to be infected. Western blot analyses of transfected cells showed that the capsid and E2 proteins were still detected after 33 days (Fig. 1b) and even after 90 days (data not shown). Similar results were obtained for NS3 (data not shown). Virus released in the supernatant of transfected cells was then used to inoculate naïve Huh-7 cells. Immunofluorescence staining revealed that a low percentage of cells was positive (Fig. 1c), but after several passages, all cells were infected (data not shown). Controls for transfection and infection were also performed with JFH-1/ΔE1-E2 and JFH-1/GND. No infection was observed with these constructs as described previously (data not shown) (Wakita *et al.*, 2005). Titration of HCV RNA by RT-qPCR assay revealed that after the first passage of transfected cells the level of detection of HCV RNA was low (Table 1). However, the extracellular HCV RNA increased slowly in the supernatant of transfected cells reaching a maximal level of $2 \times 10^6$ genome equivalent (GE) $ml^{-1}$ after four passages ($P_4$). In the same time, the infectious viral titre was only approximately $10^3$ f.f.u. $ml^{-1}$. These results indicate that our Huh-7 cells can replicate JFH-1 RNA and can be infected with HCV particles. However, in transfected cells maintained in culture, the production of infectious viral particles remained low.

### Increase in HCVcc infectivity after several rounds of infection

As a first approach, successive infections of naïve Huh-7 cells were performed to obtain higher titres of infectious virus. The scheme of infection is presented in Fig. 2. To follow the release of infectious virus particles in the supernatant, the viral RNA was extracted from supernatant and titrated by RT-qPCR. The successive infections, performed on Huh-7 cells with JFH-1 (noted $I_1$–$I_6$), led to a progressive release of viral genomes in the supernatant of inoculated cells, which reached a maximal level of $2.9 \times 10^8$ GE $ml^{-1}$ after six successive infections (Table 1). Substantially more viral RNA was released into supernatant fluids of infected cells in $I_5$ or $I_6$ than in transfected cells. Interestingly, infectious titres ranging between $10^5$ and $10^6$ f.f.u. $ml^{-1}$ were obtained at $I_5$ and $I_6$, indicating that a robust infection could be obtained with Huh-7 cell line after successive infections.

### Identification of mutations in the JFH-1 virus produced in $I_6$

Since a highly infectious JFH-1 virus was obtained after several passages, we wanted to define whether some mutations were selected during the successive infections of Huh-7 cells. To identify potential mutations in JFH-1 isolate, total cellular RNAs were prepared from infected cells in $I_6$ and the full HCV RNA genome was sequenced by RT-PCR. This approach should allow us to determine the major modifications selected during the successive infections. Surprisingly, the sequencing revealed the presence of only three mutations that were located in the E2-coding sequence. Two of them were silent mutations found at positions 1843 and 1912 (G→A and U→C). The third mutation, at position 1942 (U→A), led to a change in amino acid from Asn 534 to a Lys (N534K), which is a potential site of *N*-glycosylation (N6 site) (Fig. 3a). Thus, to verify that the core glycosylation was modified in E2 of JFH-1 produced in $I_6$, the E2 glycoprotein resulting of the first transfection was compared with that resulting of the last infection ($I_6$). As confirmed by immunoblotting, a slight shift in the E2 migration was observed (Fig. 3b, lanes $I_6$ and wt). Furthermore, no differences in the migration

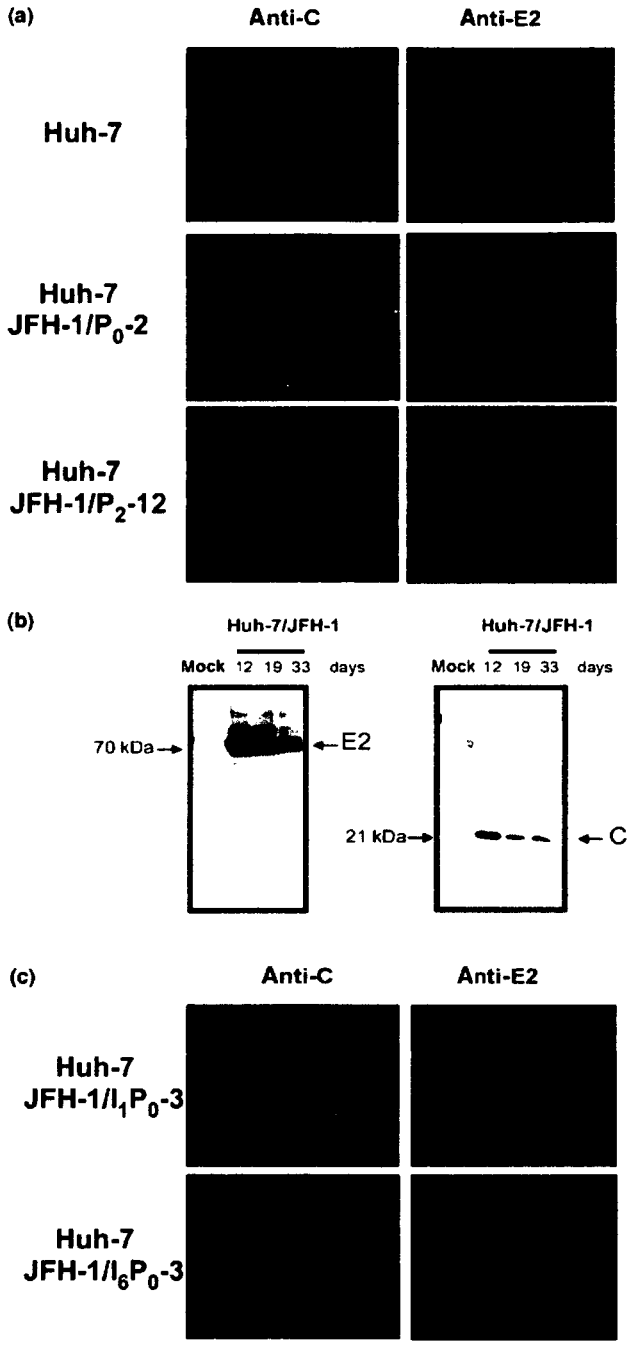


**Fig. 1.** Detection of HCV structural proteins in transfected Huh-7 cells. (a) Huh-7 cells were electroporated with the RNA transcript of JFH-1. Transfected cells grown on coverslips were fixed and processed for double-label immunofluorescence for capsid protein (green) and E2 (red) after 2 days (noted JFH-1/$P_0$-2). Transfected cells were passaged in order to maintain subconfluent cultures. After two passages transfected cells grown on coverslips were fixed and processed as described (noted JFH-1/$P_2$-12). Non-transfected Huh-7 cells were also used as control. (b) At indicated times, cell extracts were prepared and total proteins were separated by SDS-PAGE and revealed by Western blotting with mAbs ACAP27 (anti-C) and 3/11 (anti-E2). (c) Huh-7 cells were infected with supernatant of transfected or infected cells and processed 3 days later as described above (noted JFH-1/$I_1P_0$-3 and JFH-1/$I_6P_0$-3, respectively).

profiles of E2 were observed after deglycosylation by PNGase F treatment, indicating that the difference observed in the molecular mass of E2 is due to the glycosylation. Due to the higher infectious titre obtained with this final virus, we can speculate that the lack of a glycan at position N6 of E2 might favour a better interaction with an HCV receptor. Alternatively, we cannot exclude that this mutation improves the assembly and/or release of infectious particles.

## N534K mutation facilitates the infection of JFH-1 in Huh-7 cells

We focused our subsequent analyses on the role of the N534K mutation in order to determine whether this mutation may favour the infection of Huh-7 cells with JFH-1 virus. The mutation N534K was therefore introduced into the parental JFH-1 sequence. The *in vitro* transcribed recombinant JFH-1 was electroporated into the human hepatoma cells, and the ability of this virus to propagate in naïve cells was examined. As shown in Table

**Table 1.** Titration of RNA and infectious viruses during the successive infections

Evolution of RNA and infectivity titres titrated by RT-qPCR [estimated in log/genome equivalent per ml (GE $ml^{-1}$)] or determined by immunofluorescence (log/f.f.u. $ml^{-1}$) at $P_1$ of transfected or infected Huh-7 cells with JFH-1 and mutated JFH-1. Mean ± standard deviations have been calculated from three determinations. I, Infection.

| Viruses | | RNA titres log (GE $ml^{-1}$) | Infectivity titres log (f.f.u. $ml^{-1}$) |
|---|---|---|---|
| JFH-1 | / | 5.8±0.3 | 2.7±0.2 |
| | /$I_1$ | 5.9±0.2 | 2.9±0.2 |
| | /$I_2$ | 6.0±0.2 | 3.3±0.3 |
| | /$I_3$ | 6.5±0.3 | 3.7±0.2 |
| | /$I_4$ | 7.0±0.3 | 4.0±0.2 |
| | /$I_5$ | 8.1±0.3 | 5.2±0.2 |
| | /$I_6$ | 8.2±0.3 | 5.2±0.2 |
| JFH-1/N6 | / | 5.3±0.2 | 2.4±0.3 |
| | /$I_1$ | 5.7±0.3 | 2.3±0.2 |
| | /$I_2$ | 7.0±0.3 | 3.9±0.2 |
| JFH-1/CS | / | 7.0±0.3 | 3.9±0.2 |
| | /$I_1$ | 8.5±0.4 | 5.3±0.4 |
| | /$I_2$ | 9.0±0.4 | 5.8±0.2 |
| JFH-1/CS-N6 | / | 8.0±0.4 | 5.1±0.3 |
| | /$I_1$ | 8.4±0.4 | 5.7±0.3 |

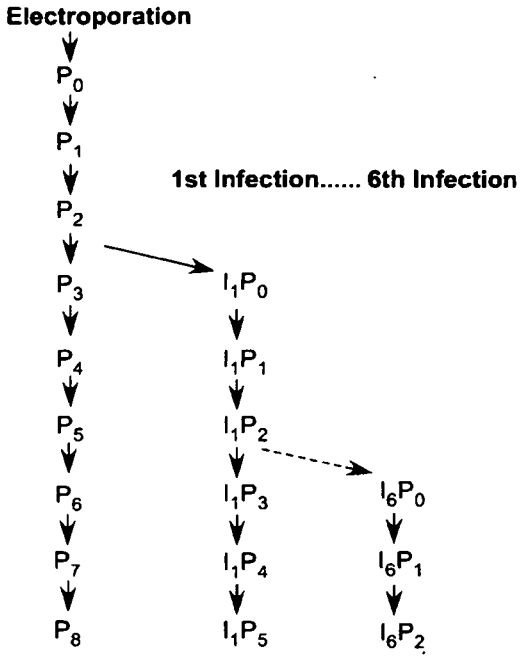


**Fig. 2.** Schematic representation of successive infections. The supernatant of transfected cells or infected cells prepared at 9–14 days was used for a new infection of naïve Huh-7 cells. Passaged transfected cells were noted P1, P2, etc., the first infection was noted $I_1$ with the corresponding passages, the second infection $I_2$ and so forth.

1, infectious virus in the supernatant of transfected cells was initially low. Indeed, the RNA and viral titres of the JFH-1/N6 (N534K) were initially comparable to the original JFH-1 virus. However, after only two successive amplifications in naïve cells, the JFH-1/N6 virus spread faster than the wild-type JFH-1 virus leading to a better production of infectious particles (Table 1). Together, these data indicate that the N534K mutation facilitates the amplification of JFH-1 virus in Huh-7 cells.

## Release of infectious particles is improved by mutations in the capsid-coding sequence

Recently, a chimeric virus containing the genotype 1a capsid-coding sequence in the context of the full-length 2a sequence [JFH-1/C(+)6-1a2a] was constructed in order to analyse the expression of F protein (D. Delgrange, T. Wakita & C. Wychowski, unpublished data). Interestingly, higher levels of infectious particles were detected in the supernatant of cells transfected with the virus JFH-1/C(+)6-1a2a ($1.5 \times 10^8$ GE $ml^{-1}$, $10^5$ f.f.u. $ml^{-1}$), suggesting that some residues present in the genotype 1a capsid protein might improve the infectivity of JFH-1. Taking advantage of this result and of previous published data with FL-J6/JFH-1 chimeric construct (Lindenbach *et al.*, 2005), the capsid-coding sequences of genotype 1a, 2a (FL-J6) and 2a (JFH-1) were aligned to identify residues that might potentially improve the JFH-1 infectivity. A sequence alignment was performed as presented in Fig. 4 and differences in the amino acid sequence of JFH-1 capsid were identified at positions 20, 48, 81, 145, 151, 152, 172 and 173. We were particularly interested by the differences

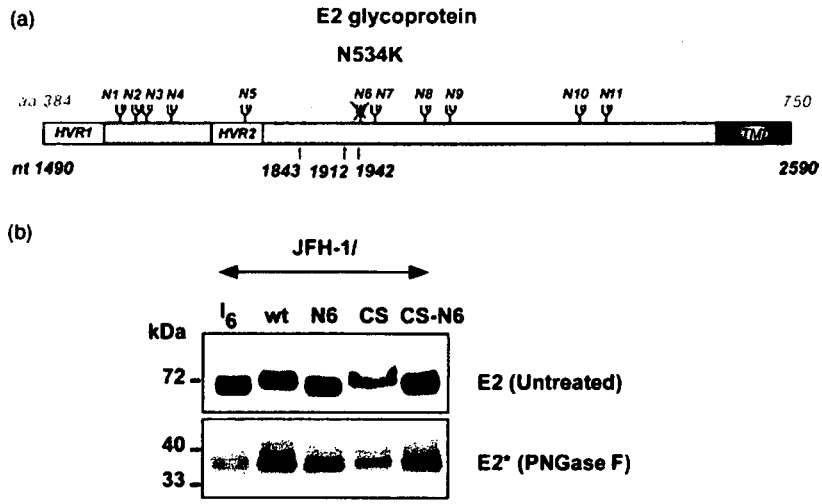


**Fig. 3.** Characterization of the N534K mutation. (a) A schematic diagram of the primary sequence of E2 glycoprotein is shown. E2 glycoprotein is located between aa 384 and 750 of JFH-1 polyprotein or between nt 1490 and 2590 of JFH-1 sequence. *N*-Glycosylated sites are indicated by branched structures and noted N1–N11. N534K is a modification of Asn→Lys residue of the glycosylation site N6 of E2. Numbers 1843, 1912 and 1942 indicate the 3 nt changes detected in the E2-coding sequence of JFH-1. (b) Analysis of glycans associated with HCV glycoprotein E2. Lysates of HCV-transfected cells [JFH-1 (wt), JFH-1/N6, JFH-1/CS and JFH-1/CS-N6] or HCV-infected cells (JFH-1/$I_6$) were prepared and total proteins were immunoprecipitated with anti-E2 mAb AP33. The immunoprecipitates were then treated or not treated with PNGase F. Proteins were separated by SDS-PAGE and then revealed by Western blotting with the anti-E2 mAb 3/11. E2* represents the unglycosylated protein.

```
                1                                                  50
HCV-H77         MSTNPKPQRK  TKRNTNRRPQ  DVEFPGGGQI  VGGVYLLPRR  GPRLGVRATR
HCV-J6          MSTNPKPQRK  TKRNTNRRPQ  DVKFPGGGQI  VGGVYLLPRR  GPRLGVRATR
HCV-JFH-1       MSTNPKPQRK  TKRNTNRRPE  DVKFPGGGQI  VGGVYLLPRR  GPRLGVRTTR
               51                                                 100
HCV-H77         KTSERSQPRG  RRQPIPKARR  PEGRTWAQPG  YPWPLYGNEG  CGWAGWLLSP
HCV-J6          KTSERSQPRG  RRQPIPKDRR  STGKSWGKPG  YPWPLYGNEG  LGWAGWLLSP
HCV-JFH-1       KTSERSQPRG  RRQPIPKDRR  STGKAWGKPG  RPWPLYGNEG  LGWAGWLLSP
              101                                                 150
HCV-H77         RGSRPSWGPT  DPRRRSRNLG  KVIDTLTCGF  ADLMGYIPLV  GAPLGGAARA
HCV-J6          RGSRPSWGPN  DPRHRSRNVG  KVIDTLTCGF  ADLMGYIPVV  GAPLGGVARA
HCV-JFH1-1      RGSRPSWGPT  DPRHRSRNVG  KVIDTLTCGF  ADLMGYIPVV  GAPLSGAARA
              151                                 191
HCV-H77         ALHGVRVLED  GVNYATGNLP  GCSFSIFLLA  LLSCLTVPASA
HCV-J6          ALHGVRVLED  GVNFATGNLP  GCSFSIFLLA  LLSCITTPVSA
HCV-JFH-1       VAHGVRVLED  GVNYATGNLP  GFPFSIFLLA  LLSCITVPVSA
```

**Fig. 4.** Alignment of amino acids of capsid proteins of genotype 1a and 2a. The sequences of amino acids corresponding to the genotype 1a (HCV-H77) and genotype 2a (HCV-J6 and HCV-JFH-1) were aligned. The boxes indicate modifications that were detected in JFH-1 but not in strains J6 and H-77.

in amino acids at positions 172 and 173 because they correspond to drastic mutations in the context of JFH-1. Furthermore, another study relating to the genotype 2a capsid protein has shown that some modifications in the C-terminal 31 aa of core protein were important for its processing and/or its morphogenesis (Kato *et al.*, 2003b). Consequently, the mutations F172C and P173S (FP→CS) were introduced by site-directed mutagenesis in JFH-1 capsid-coding sequence to determine whether the release of infectious viral particles could be improved (Fig. 5a). HCV RNA was quantified and the secretion of particles was analysed by successive passages of the transfected cells or by successive infections on naïve Huh-7 cells as initially described in this study (Table 1). High viral titres of JFH-1/CS were obtained faster and were higher than those obtained with JFH-1. These data suggest that the replacement of FP to CS residues confers an advantage for the virus and these modifications might improve the morphogenesis and/or the release of viral particles.

A previous study has shown that the capsid protein and E2 glycoprotein do not colocalize in JFH-1 infected cells (Rouille *et al.*, 2006). We next wanted to determine whether the JFH-1/CS mutant might affect the subcellular localization of the capsid protein, leading to some colocalization with the envelope proteins. As shown in Fig. 5(b), no differences were observed between the two viruses in the intracellular distribution of the capsid protein and E2 glycoprotein. For both clones, E2 colocalized with ER markers, whereas capsid protein was associated with lipid droplets (data not shown). In addition, no differences were observed in the capsid protein when analysed by Western blotting (Fig. 5c). Consequently, no detectable differences in the capsid processing and intracellular localization were observed that could explain the enhanced production of viral particles.

## N534K, F172C and P173S mutations improve the infection of JFH-1 in Huh-7 cells

In order to produce a higher infectious JFH-1 virus in cell culture, we introduced three mutations N534K, F172C and P173S into JFH-1 (JFH-1/CS-N6). Moreover, to visualize more efficiently the infectivity of this mutant on cell culture, Huh-7 cells were transfected with the *in vitro* transcribed JFH-1, JFH-1/N6, JFH-1/CS and JFH-1/CS-N6 RNAs (Fig. 6a) and the supernatants obtained at 3 days post-transfection were used in the infection of naïve Huh-7

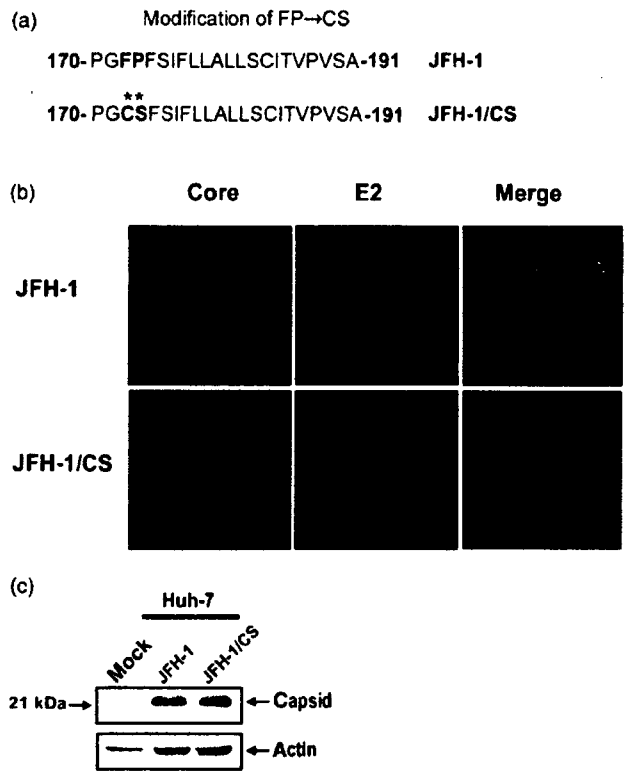


**Fig. 5.** Some characteristics of JFH-1/CS virus. (a) Modifications introduced in the capsid protein of JFH-1. The numbers at each side indicate the location of the first and last amino acid in the sequence. (b) Intracellular localization of HCV capsid and E2 proteins analysed by confocal immunofluorescence microscopy on cells infected either by JFH-1 or JFH-1/CS. (c) Total proteins of lysates of Huh-7 cells infected with JFH-1 or JFH-1/CS were separated by SDS-PAGE and revealed by Western blotting with the anti-C mAb ACAP27. Then, the membrane was stripped and processed for the detection of actin used as control.

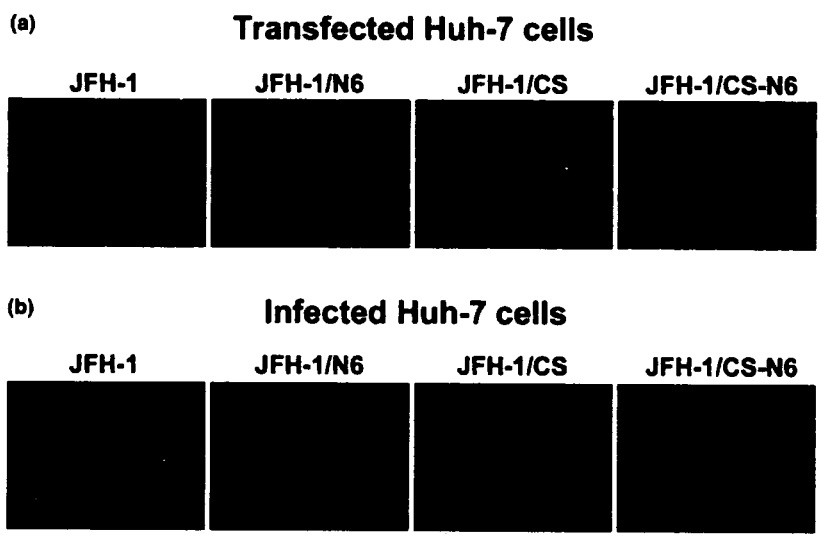


**Fig. 6.** Comparison of infectivity of each mutant by immunofluorescence. (a) Huh-7 cells were electroporated with RNA transcripts of JFH-1, JFH-1/N6, JFH-1/CS and JFH-1/CS-N6. Transfected cells were grown on coverslips. After 3 days, the cells were fixed and processed for double-label immunofluorescence for capsid protein (green) and nuclei (blue, Hoescht). (b) Naïve Huh-7 cells seeded on coverslips were infected with the supernatant obtained at 3 days post-transfection, and then fixed and processed at 3 days post-infection for double-label immunofluorescence for capsid protein (green) and nuclei (blue, Hoescht).

cells (Fig. 6b). The profile of E2 produced by each virus was also analysed before and after treatment with PNGase F and was consistent with predicted results (Fig. 3b). Our results suggest that the JFH-1/CS-N6 virus expands more rapidly and reaches higher titres than the JFH-1, JFH-1/N6 and JFH-1/CS viruses (Fig. 6b and Table 1). As for JFH-1/CS, no differences were observed in the intracellular distribution of the capsid protein and E2 glycoprotein of JFH-1/CS-N6 (data not shown). Furthermore, we also observed that after a single round of amplification the JFH-1/CS-N6 virus displayed an accelerated cytopathic effect, which was faster than what we observed for the JFH-1/CS virus (data not shown). These data suggested that the combined mutations located in the capsid- and E2-coding sequences resulted in an enhanced virus infectivity.

## DISCUSSION

Although a low efficiency of infection has been detected by transfection of Huh-7 cells with the RNA generated from a genomic JFH-1 viral clone, this discovery has been a major breakthrough in HCV research (Wakita *et al.*, 2005). Different groups have developed robust cell culture systems for the propagation of HCV, and the data led to the conclusions that the Huh-7 cell culture is important for the propagation of the virus and that each Huh-7 cell line can display different permissiveness to the virus. In this study, we established a strong production of infectious HCV particles by using successive infections of naïve Huh-7 cells or by introducing specific mutations into the JFH-1 genome.

Contrary to what was observed in other groups (Lindenbach *et al.*, 2005; Zhong *et al.*, 2005), the robust production of HCVcc in our Huh-7 cell line was only obtained after several successive infections. Initially, the JFH-1 virus released into the culture medium after the first transfection was low, which was consistent with a previous report (Wakita *et al.*, 2005). It is worth noting that several passages of transfected cells did not change the viral titre. However, after repeated infections of naïve Huh-7 cells, analyses of HCV RNA in the medium of infected cells revealed an increase in the particle release, which was correlated with a higher titre of infectious virus. The direct sequencing of HCV RNA genome was used to determine the major modifications appearing in JFH-1. Surprisingly, the only coding mutation identified was an Asn to Lys mutation located at aa 534 (N534K) in E2. This modification, which is characterized as preventing the addition of an *N*-glycan at the E2 glycosylation site 6, may favour the interaction between HCV E2 glycoprotein and a cellular receptor. Indeed, the introduction of this mutation in JFH-1 leads to a higher infectious titre after only two successive infections. This suggests that the particles produced by JFH-1/N6 are more effective than those produced by JFH-1 for the reinfection of Huh-7 cells. This is also true when the mutation N534K is combined with the modifications FP→CS at positions 172 and 173 in JFH-1 (Fig. 6b). Consequently these mutations might lead to a better viral expansion on Huh-7 cells. There is some evidence that CD81 is essential for the entry of HCVpp (Hsu *et al.*, 2003; Lavillette *et al.*, 2005) or HCVcc (Lindenbach *et al.*, 2005; Zhong *et al.*, 2005) into hepatoma cells via an interaction with the HCV E2 glycoprotein (Pileri *et al.*, 1998). Residues critical for the CD81 binding have been identified in the HCV glycoprotein E2. These residues are located at positions 420, 437, 438, 441, 442, 529, 530 and 535 of E2 glycoprotein (Drummer *et al.*, 2006; Owsianka *et al.*, 2006). Moreover, replacement of Thr at the E2 glycosylation site 6 results in moderately increased CD81 binding (Owsianka *et al.*, 2006). This is consistent with the hypothesis that the loss of the *N*-linked E2 glycosylation site 6 favours a better exposure of E2 to the E2-binding site of CD81 and then the JFH-1 reinfection. In a similar way, Zhong *et al.*, (2006)